NUCLEAR PARTICLE PHYSICS WITH eA AT THE LHeC/FCC-eh*

Anna M. Staśto

Department of Physics, Penn State University, University Park, PA 16802, USA

Received 30 April 2023, accepted 12 May 2023, published online 6 September 2023

Large Hadron electron Collider (LHeC) and its more energetic counterpart, the Future Circular electron–hadron Collider (FCC-eh), are proposals for next-generation Deep Inelastic Scattering facilities at CERN. Both experiments would perform electron–proton and electron–nucleus collisions at high energy and luminosity. In this paper, I present an overview of the possibilities for exploring nuclear physics with eA collisions at the LHeC and FCC-eh.

DOI:10.5506/APhysPolBSupp.16.7-A23

1. Introduction

The Deep Inelastic Scattering (DIS) of leptons off nuclei offers a unique opportunity for exploration of the nuclear structure. The DIS process allows for the detailed mapping of nuclear structure in the wide range of (x, Q^2) plane, where x is the longitudinal momentum fraction of the nucleon carried by the struck parton, and Q^2, the (negative) boson virtuality exchanged between the lepton and the quark from the nucleus. It allows for the precise measurements of the nuclear structure functions and extraction of the nuclear parton distribution functions, nPDFs. These quantities are important and interesting on their own as they encode information about the fundamental structure and dynamics of nuclei probed at high energies but are also necessary for a precise description of the initial state in the heavy-ion collisions. In the latter context, the eA measurements are invaluable to benchmark and test the assumptions about the validity of the factorization description in pA and AA collisions of processes involving hard scales. In addition, eA collisions can provide information for the understanding of cold matter modifications of QCD radiation and hadronisation, which will then allow for the comparison of these effects due to the creation of deconfined

* Presented at the 29$^{\text{th}}$ Cracow Epiphany Conference on *Physics at the Electron–Ion Collider and Future Facilities*, Cracow, Poland, 16–19 January, 2023.

medium in AA collisions. The eA collisions at high energy and for large nuclei offer an unprecedented opportunity to explore the novel regime of QCD, which is expected to set in at high collision energies. The onset of high gluon densities is anticipated on general grounds from the theoretical analysis of the high-energy limit of QCD which predicts the existence of the characteristic dynamical scale, the saturation scale, that divides the dilute and dense regions. In the latter, the QCD evolution equations for the parton densities need to be supplemented by the non-linear terms which lead to the parton saturation phenomenon and are aiding to restore the unitarity of the cross sections. Diffractive phenomena in eA, which are mediated by the colourless exchange, an object mostly composed of gluons, could also be explored in eA, and they offer a unique window into the novel small-x dynamics as well as nuclear shadowing. Nuclear diffractive parton distributions, which can be interpreted as conditional probabilities for finding a parton in a nucleus, provided the nucleus stays intact, would be extracted for the first time at the LHeC or FCC-eh. The exclusive diffractive processes, particularly of the vector mesons, allow for the mapping of the spatial distribution of the gluons in nucleons and nuclei, and also provide the tests of the onset of the saturation. Finally, hadronization and fragmentation could be measured in eA and depending on the energy of the parton various scenarios can be tested which could distinguish between in- or out-medium hadronization. These studies can have a crucial impact on the physics explored in high-energy heavy-ion collisions.

Large Hadron-electron Collider or LHeC [1, 2] is a proposed next generation high-energy DIS machine that will be capable of colliding electrons with protons and nuclei. The electrons would be accelerated in the Energy Recovery Linac (ERL) up to about 50–60 GeV and then collided with the protons or nuclei from the LHC. The nuclear beams from the LHC would reach the energy of 2.75 TeV per nucleon, thus resulting in centre-of-mass energy of $\sqrt{s} = 812$ GeV. The integrated luminosity for collisions on nuclei at LHeC is projected to be of the order of 10 fb^{-1} which is ten times larger than the total luminosity collected in ep collisions at HERA. Further in the future, the Future Circular Collider [3, 4] in electron–hadron option, FCC-eh, would be the next generation facility, colliding electrons from the ERL with the protons or nuclei from the FCC. The attainable energies would be 50 TeV for protons and 19.7 TeV per nucleon for lead nuclei.

These two proposals are complementary to a current DIS project that is being realized, the Electron Ion Collider (EIC) [5, 6] in the U.S. at Brookhaven National Laboratory. This machine will collide electrons with a wide range of nuclei, with high luminosity, and at varying centre-of-mass energies, from 20 to 140 GeV. It will also have polarized electron and nucleon beams and the possibility of polarized light ions. All three machines are unique and complementary in their physics goals.

2. Inclusive DIS

2.1. Nuclear structure functions

The DIS cross section for electron–hadron(nucleus) in the unpolarized case and the one-photon exchange approximation has the following form:

$$\frac{\mathrm{d}^2\sigma}{\mathrm{d}x\,\mathrm{d}Q^2} = \frac{2\pi\alpha_{\mathrm{em}}^2}{xQ^2}\, Y_+\, \sigma_{\mathrm{r}}\left(x, Q^2\right) , \tag{1}$$

where the reduced cross section σ_{r} can be written in terms of two dimensionless structure functions $F_2(x, Q^2)$ and $F_L(x, Q^2)$

$$\sigma_{\mathrm{r}}\left(x, Q^2\right) = F_2\left(x, Q^2\right) - \frac{y^2}{Y_+} F_L\left(x, Q^2\right) , \tag{2}$$

where $Y_+ = 1 + (1 - y)^2$ and y is inelasticity of the electron.

The nuclear effects for the eA scattering can be illustrated by examining the ratio of the structure functions

$$R_{2,\mathrm{L}}^A\left(x, Q^2\right) = \frac{F_{2,\mathrm{L}}^A\left(x, Q^2\right)}{A\, F_{2,\mathrm{L}}\left(x, Q^2\right)} , \tag{3}$$

where $F_{2,\mathrm{L}}$ are structure functions for the proton and $F_{2,\mathrm{L}}^A$ are structure functions for the nucleus with mass number A.

When the nuclear ratio in Eq. (3) is different from unity, this indicates the nuclear effects. For a fixed value of Q^2, the ratio has a complicated x dependence, which can be divided roughly into several regions: *(i)* $x \geq 0.8$, the Fermi motion region; *(ii)* $0.25 \div 0.3 \leq x \leq 0.8$, the EMC region; *(iii)* $0.1 \leq x \leq 0.25 \div 0.3$, the antishadowing region; *(iv)* $x \leq 0.1$, the shadowing region. The ratio also changes with Q^2 and A, and its measurement provides an opportunity to test various models aiming to describe underlying physics in different regions.

The LHeC and FCC-eh machines, thanks to their high energy, will extend the existing range of data in (x, Q^2) for nuclear structure function up to 4–5 orders in magnitude. The kinematic coverage of both machines is illustrated in Fig. 1. Also shown in this figure is the range which can be explored in the pA collisions at the LHC and dA collisions at RHIC. Although LHC in the pA mode can have access to nuclear parton distributions at large scales and also at small x, DIS offers a very clean experimental environment characterized by low multiplicity, no pileup, and fully constrained kinematics. On the theory side, in DIS, there exist many first-principles calculations in collinear and non-collinear frameworks. Therefore, eA collisions offer full complementarity to the pA and also ultraperipheral collisions (UPC). In addition to fully inclusive structure functions, the LHeC and FCC-eh machines

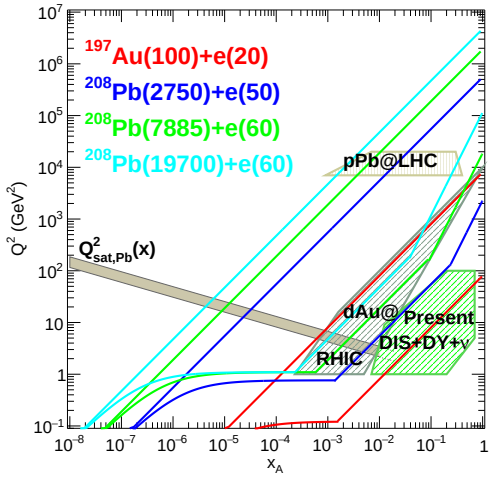

Fig. 1. (Colour on-line) Kinematic plane (x, Q^2) at the LHeC (dark blue) and two FCC-eh versions $E_N = 7.885$ TeV (green) and $E_N = 19.7$ TeV (light blue). Indicated are also available measurements (charged lepton and neutrino DIS, DY, dAu at RHIC and pPb at the LHC), as well as the projected range of the EIC (red), Also drawn is the projected saturation scale $Q_{\rm sat}$. Figure from [2].

will be able to measure with high precision the charm and beauty structure functions. In Fig. 2, a sample set of pseudodata for the charm structure function F_{2c} as a function of Q^2 and for different values of x is shown with projected statistical and systematic uncertainties.

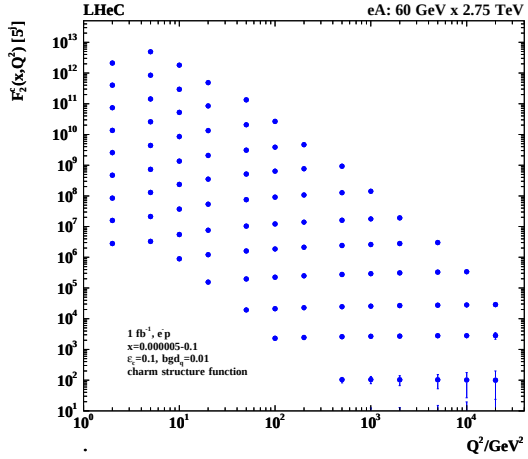

Fig. 2. Pseudodata with projected systematic and statistical uncertainties for the F_2^c charm structure function in eA scattering at the LHeC. Figure from [2].

2.2. Nuclear parton distribution functions

From the inclusive structure function measurements, one can extract nuclear parton distribution functions, nPDFs. They not only contain crucial information about the structure of nuclei but also allow for the predictions of other processes with hard scales, using the collinear factorization framework. Since structure functions in nuclei are modified with respect to the proton case and cannot be taken as simple superpositions of the proton structure functions, the resulting nuclear parton density functions will contain nuclear modifications, which can be quantified by the analogous ratios (*i.e.* compare Eq. (3))

$$R_i\left(x,Q^2\right)=\frac{f_i^A\left(x,Q^2\right)}{Af_i^p\left(x,Q^2\right)}\,,\qquad i=g,u,d,s,c,\bar{u},\bar{d},\bar{s},\bar{c},\ldots \tag{4}$$

In the standard collinear approach, the nuclear effects are encoded in the non-perturbative initial conditions at some low scale Q_0^2. Since the data on nuclear structure functions are not as abundant as in the proton case, there are large uncertainties in the nuclear PDFs, especially in the low-x region, which is the region of nuclear shadowing. In Fig. 3, the results of the simulation, extracting the nuclear PDFs from the fits to the LHeC and FCC-eh pseudodata are shown. The fits have been performed to NC+CC LHeC/FCC-eh pseudodata for $Q^2 > 3.5$ GeV^2. The same proton parametrisation was used, both for pseudodata simulation (hence the nuclear ratio is one in this model) and fit extraction. Neither theoretical uncertainties nor the uncertainty related to the functional form of the initial condition were considered in this study. Therefore, this analysis provides an estimate of possible experimental precision in the extraction of nPDFs. As is evident from Fig. 3, great improvement in the precision of the extracted nuclear PDF is possible both for LHeC and FCC-eh, particularly in the small-x region. Further improvements are possible, by performing more differential studies, for example, by taking into account charm or bottom structure functions and performing simultaneous fits to F_2^A and F_{2c}^A, which can give more constraints on the gluon distribution. If the centre-of-mass energy can be varied, the longitudinal structure function F_{L} can be extracted and would provide valuable information on the gluonic content of the proton, and can help constrain the models of the parton evolution at low x and low Q^2.

To summarize, using the inclusive DIS with nuclei at the LHeC and FCC-eh, one can perform precise extraction of the PDFs of a single nucleus with full flavor decomposition, as in the case of the protons. The nuclear effects can be more easily quantified since the same machine will be used to perform the measurements on protons, and hence one can use the same extraction of the PDFs from protons and nuclei. Physics beyond the standard collinear factorisation can be studied in a single setup, with a large lever arm in x and in Q^2 with size effects disentangled from the energy effects.

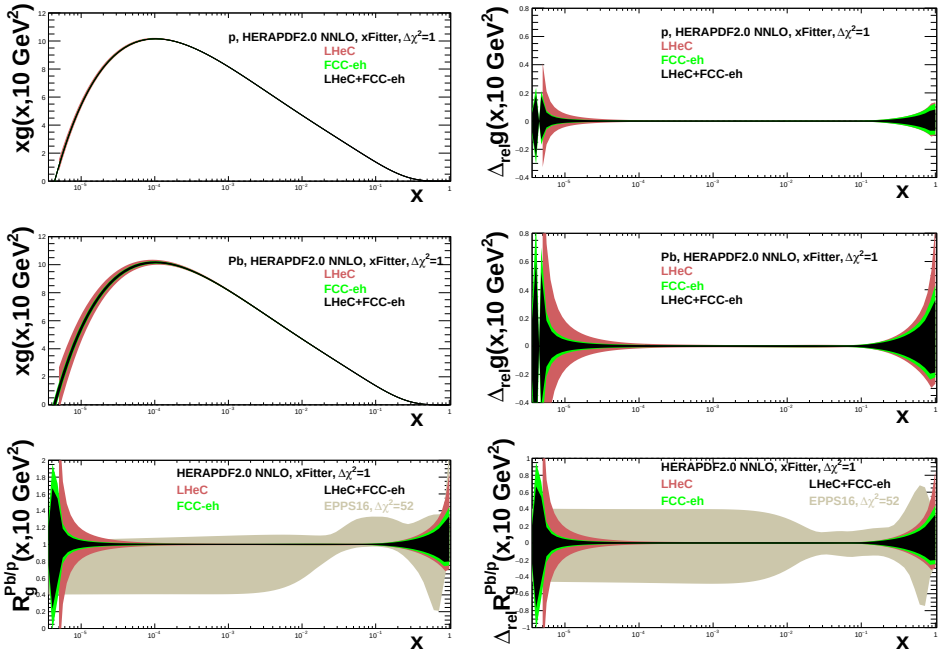

Fig. 3. Gluon distributions (left) and their relative uncertainties (right). Top: gluon density in the proton. Middle: gluon density in Pb. Bottom: nuclear modifications factor in the analysis of ep and ePb LHeC and FCC-eh pseudodata using xFitter code. Figure from [2].

3. Novel small-x dynamics in nuclear environment

It is well known that the increase of the structure functions with decreasing x is driven by the increase of the gluon density through the mechanism of the gluon splitting. At fixed values of Q^2, the gluon evolution with $\ln 1/x$ is described by the linear Balitsky–Fadin–Kuraev–Lipatov (BFKL) evolution which leads to the very strong increase of the density. Thus, the standard evolution based on the Dokshitzer–Gribov–Lipatov–Altarelli–Parisi (DGLAP) linear equations needs to be modified to include the effects of the resummation of large $\ln 1/x$. Furthermore, since the densities are very high, there will be a competing mechanism that needs to be included, and that is of the gluon recombination. When this effect is important, QCD predicts that the novel regime will be attained at small x, the gluon saturation. Since this is a density effect, the non-linear evolution may become important when the mass number is increased. This means that the non-linear regime may be achieved by either decreasing x or by increasing A or some combination of the two. Since LHeC and FCC-eh are both high-energy machines,

which will explore the region of small x and, at the same time, capable of performing collisions of electrons with heavy nuclei, parton saturation may be tested using the two-pronged approach.

QCD in the limit of high energy and density predicts the existence of the saturation scale, the dynamically generated energy-dependent scale which delineates the boundary between the dilute and dense regimes. Roughly speaking, it can be cast into the following, simplified form:

$$Q_{\mathrm{s}}^2(x, A) \simeq Q_0^2 \left(\frac{x}{x_0}\right)^{-\lambda} A^{1/3}\,, \tag{5}$$

with the power $\lambda \simeq 0.3$. The saturation scale in principle depends very strongly on the impact parameter, thus the quantity above is understood in an average sense. When transverse scales are smaller than the saturation scale, the evolution of the gluon density needs to include the non-linear terms in gluon density. Thus, the nature of the evolution changes and the boundary between dilute and dense regimes is given by the saturation scale. The theory predicts the energy dependence of the saturation scale, but the normalization has to be fixed from the experiment. Both LHeC and FCC-eh offer a long lever arm in $\ln 1/x$ and $\ln Q^2$, as well as the possibility of running with nuclei and thus the saturation can be tested in these machines. In practice, extraction of the saturation scale from the inclusive structure functions proved to be notoriously difficult because there is large flexibility in the initial conditions for the linear evolution, and hence at least some (or a large part of) non-linear effects can be hidden in the non-perturbative initial conditions for the linear evolution. This was explored in the analysis of Ref. [7] which focused on quantifying the differences between linear and non-linear evolution. Matching was performed in the region where both frameworks are expected to provide a good description of the parton dynamics. Then, the differences were quantified by the deviations in the results when moving away from the matching region. The results are shown in Fig. 4 for $A = 197$ in the form of the relative difference

$$\mathcal{R}_{2,\mathrm{L}} \equiv \frac{F_{2,\mathrm{L}}^{\mathrm{sat}} - F_{2,\mathrm{L}}^{\mathrm{lin}}}{F_{2,\mathrm{L}}^{\mathrm{sat}}}\,, \tag{6}$$

where F^{sat} and F^{lin} are the structure functions obtained from the non-linear and linear approaches. The left plot indicates the results for the case of F_2 and the right plot indicates the results for F_{L}. It was found that, for LHeC and FCC-eh, the differences for nucleus in F_2 reach about 10%, and 60% for F_{L}. In the case of the proton, these differences are smaller, since for F_2 are at the level of a few percent and for F_{L} up to 40%. This demonstrates that both LHeC and FCC-eh will have the potential to discover and quantify

the saturation effects in heavy nuclei and that the longitudinal structure function is much more sensitive to these effects, indicating that it may be a necessary observable in the case of scattering off the protons.

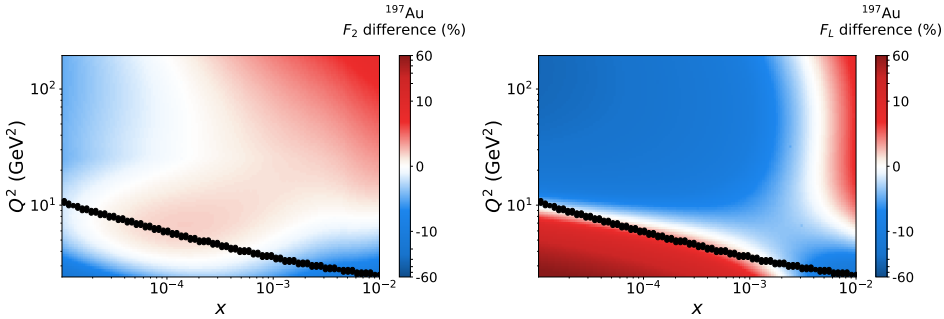

Fig. 4. Relative difference, ratio $\mathcal{R}_{2,\mathrm{L}}$ Eq. (6) between the structure functions F_2 (left plot) and F_L (right plot) for $A = 197$ as a function of x and Q^2. The black line indicates the matching of two calculations. Figure from [7].

4. Diffraction

At electron–proton HERA collider about 10% of DIS events were diffractive, that is they were characterized by the presence of a large rapidity gap. The rapidity gap is the region in the detector with no activity in an event. In the diffractive process, $e + p \to e + p(Y) + X$, see Fig. 5, the incoming hadron (proton or a nucleus) undergoes elastic scattering, or is dissociated into a low-mass excitation Y with the same quantum number. The diffractive mass X is well separated from the proton or its remnants. In the case of scattering off nuclei, diffraction becomes a more involved process than in the proton case because in addition to coherent process $e + A \to e + A + X$ with an intact nucleus in the final state (see the left plot of Fig. 5 with the replacement $p \to A$), there is also incoherent $e + A \to e + A^* + X$ diffraction, where A^* is an excited nuclear state (see the right plot of Fig. 5). This puts additional constraints on the detector design, as the two classes of events should be distinguished for a meaningful comparison with the theoretical calculations.

In order for the rapidity gap to exist, the diffractive process has to be mediated by an exchange of the colorless state with quantum numbers of the vacuum which traditionally is referred to as the *Pomeron*. Since this exchange has to be colourless, studying the diffraction and the Pomeron can offer insight into the relation with the confinement mechanism in QCD. Diffraction can also provide the details into the gluon dynamics at low values of Bjorken x and the onset of the non-linear evolution. In the context of

nuclei, the diffraction is also known to be related to the mechanism of nuclear shadowing. Exclusive diffractive processes can be used to infer the details of the structure of protons and nuclei in impact parameter space.

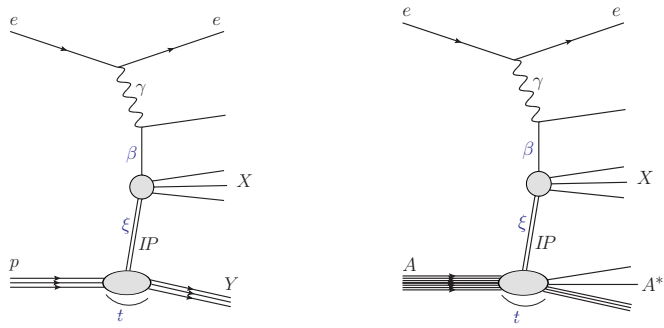

Fig. 5. Left: diffractive process in DIS. Y is either the elastically scattered proton or a low-mass excitation, IP is the colour singlet exchange ('Pomeron'), and X is the diffractive mass. Kinematic variables: t — momentum transfer at the proton vertex, ξ — longitudinal momentum fraction of the proton carried by the Pomeron, and β — longitudinal momentum fraction of the Pomeron carried by the parton. Right: incoherent diffraction on nuclei. The final state A^* can be a nucleus in an excited state which can further disintegrate into another nucleus and any number of nucleons.

In Fig. 6, simulated data for reduced diffractive cross section in eA are presented for the LHeC (left) and FCC-eh (right) scenarios assuming 5% uncorrelated systematic error and 2 fb^{-1} integrated luminosity. The projected precision of the data is very high and comparable to the proton case [9]. Thus, it can be concluded that a very accurate measurement of the nuclear diffractive cross section would be possible in the eA case at both LHeC and FCC-eh, and thus it will be possible to extract the nuclear diffractive PDFs with very high accuracy for the first time.

In addition to inclusive diffraction, the exclusive diffractive phenomena offer new possibilities, in particular, allowing for the precise mapping of the spatial distribution in nuclei. The important process in this class is the exclusive diffractive production of vector mesons. This process is particularly sensitive to the gluon distribution at low x since, roughly speaking, it depends on the square of the gluon density. The measurement of the energy dependence in this process can thus provide information about the onset of the nonlinear evolution in the gluon density. The momentum transfer dependence in the differential cross section can be used to map the spatial structure of the hadronic target. The extended kinematic range of LHeC and FCC-eh will allow to study the details of this process as a function of energy, momentum transfer, and photon virtuality, and test the QCD mod-

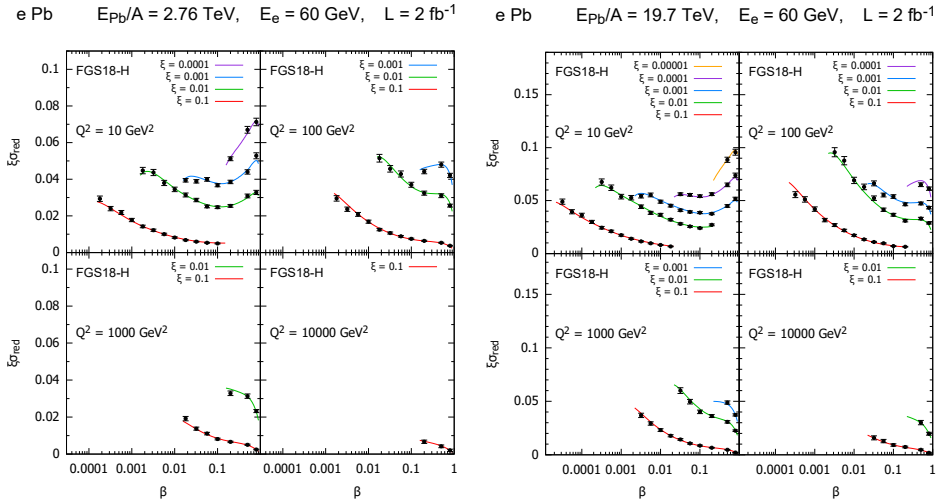

Fig. 6. Simulated data for the diffractive reduced cross section as a function of β in bins of ξ and Q^2 for ePb collisions at the LHeC (left plot) and FCC-eh (right plot) using the model of [8]. Figure from [9].

els, which predict the dependence of the cross section in this process on the interplay of these three variables. In the case of nuclei, this process does present experimental challenges, since one needs to distinguish between coherent and incoherent diffraction. Thus, dedicated forward instrumentation which will allow disentangling these two cases is needed.

5. Conclusions

LHeC and FCC-eh will explore new territory in (x, Q^2) kinematic plane in DIS with nuclei. Precise determination of nuclear PDFs will be possible, and tests of onset of the saturation at low x and varying A. High energy and luminosity of these machines will allow for precision physics with heavy flavors. Measurements of the inclusive diffraction will allow for the extraction of nuclear diffractive PDFs for the first time. Exclusive diffractive processes with vector mesons would allow to explore the nuclear structure in impact parameters. In addition, many other processes can be studied, such as azimuthal decorrelations of hadrons, with sensitivity to parton saturation, and semi-inclusive production of hadrons which will allow for the study of nuclear effects on radiation, fragmentation, and hadronization.

The author is supported in part by the U.S. Department of Energy grant DE-SC-0002145 and within the framework of the Saturated Glue (SURGE) Topical Theory Collaboration.

REFERENCES

[1] J.L. Abelleira Fernandez *et al.*, *J. Phys. G: Nucl. Part. Phys.* **39**, 075001 (2012).

[2] P. Agostini *et al.*, *J. Phys. G: Nucl. Part. Phys.* **48**, 110501 (2021).

[3] FCC Collaboration (A. Abada *et al.*), *Eur. Phys. J. C* **79**, 474 (2019).

[4] FCC Collaboration (A. Abada *et al.*), *Eur. Phys. J. Spec. Top.* **228**, 755 (2019).

[5] A. Accardi *et al.*, *Eur. Phys. J. A* **52**, 268 (2016).

[6] R. Abdul Khalek *et al.*, *Nucl. Phys. A* **1026**, 122447 (2022).

[7] N. Armesto *et al.*, *Phys. Rev. D* **105**, 114017 (2022).

[8] L. Frankfurt, V. Guzey, M. Strikman, *Phys. Rep.* **512**, 255 (2012).

[9] N. Armesto, P.R. Newman, W. Słomiński, A.M. Staśto, *Phys. Rev. D* **100**, 074022 (2019).